Journal of Manufacturing Processes 84 (2022) 1094–1102

Contents lists available at ScienceDirect

Journal of Manufacturing Processes

journal homepage: www.elsevier.com/locate/manpro

Build orientation optimization of additive manufactured parts for better mechanical performance by utilizing the principal stress directions

Márton Tamás Birosz *, Ferenc Safranyik, Mátyás Andó

Eötvös Loránd University, Faculty of Informatics, Savaria Institute of Technology, Hungary

ARTICLE INFO

Keywords:
Additive manufacturing
Build orientation
FEA
Anisotropy
Optimization

ABSTRACT

As Additive Manufacturing technology is excellent for the production of function-based optimized parts. By choosing the right printing orientation, the dimensional accuracy and surface quality of the parts can be improved. But also possible to achieve improvement of the mechanical properties by the proper orientation. An algorithm has been developed, which can determine the optimal build orientation based on a numerical simulation for a given load case. The adverse and favourable load directions can be defined according to the layer's position by knowing the anisotropic behavior of the printed parts. The optimal print orientation has been found for four investigated geometries, according to the No-Preference and Weighted Sum multiple-objective optimization methods, and therefore the expected mechanical performance was increased. The algorithm was able to reduce the amount of unfavourable stresses by 100 % for simple beam geometries with longitudinal tensile and compression loads, while the more complex geometries were improved to the best possible extent.

1. Introduction

The shape-forming freedom provided by Additive Manufacturing (AM) gives an outstanding new design attitude for engineers. Nowadays, the parts created by AM not only serve as a result product of Rapid Prototyping (RP) but mainly serve as fully functional end products. By exploiting the merits of AM and with the combination of different CAD/CAE solutions the function optimized structures can easily be achieved with only minor restricting concerns. The AM technologies all share the layered shape forming procedure, as they build up the part additively layer upon layer [1,2]. The standard, ISO/ASTM 52900:2015 Additive manufacturing – General principles – Terminology, classifies the different technologies into seven categories. Among them, two suffer the significant adverse effect of mechanical anisotropy resulting from layering. These categories are namely the Material Extrusion (ME) and Direct Energy Deposition (DED) techniques. The other techniques also share some adverse effects of layering, but since the forming mechanism differs the significance of the anisotropy is less. It is a crucial step to adjust the printing technology for the expected performance of the part for ME and DED. It can be reached by modifying the toolpath for the 3D printing technology, for example, by using a multi-axis tool to bridge the 2,5D build logic [3,4]. Another and more frequently used solution is to simply select the build orientation to achieve the best possible mechanical performance, e.g. higher stiffness [5,6], as well as some other parameters like surface roughness and dimensional accuracy [7,8]. The consideration of the layering can be done during the design process, but the rotation of the part helps to get the best position [9,10]. However, aware of the layering the volume minimization of the structure can be tuned for example in the case of Topology Optimization (TO), Generative Design, or Functionally Graded Lattice Structures (FGLS), as they are popular research trends for AM [11].

The anisotropic behavior of the ME and DED parts is typically described by an orthotropic material model, as it can distribute the emerged stresses on three orthogonal axes [12,13]. These axes are usually identical to the Cartesian coordinates of the build domain of the 3D printing. From numerous published research works [14–16], it can be stated, that the anisotropy of the parts can be divided into two decisive directions. The investigated AM processes show an effect mainly along the direction of normal to the build tray (Z direction). Therefore, the coordinate axes, which define the printing plane (X and Y direction) share the same mechanical properties (Young's modulus, Tensile modulus, Poisson ratio). Furthermore, the parts with applied loads perpendicular to the layers (Z direction) show the least mechanical resistance, thus they can fail easily. The parts whose load direction lay in the X-Y plane have better possible resistance. The transition between these two loads perpendicular to each other can be affected by many

* Corresponding author.
E-mail address: birosz.marton@gmail.com (M.T. Birosz).

https://doi.org/10.1016/j.jmapro.2022.10.038
Received 25 July 2022; Received in revised form 1 October 2022; Accepted 13 October 2022
Available online 5 November 2022

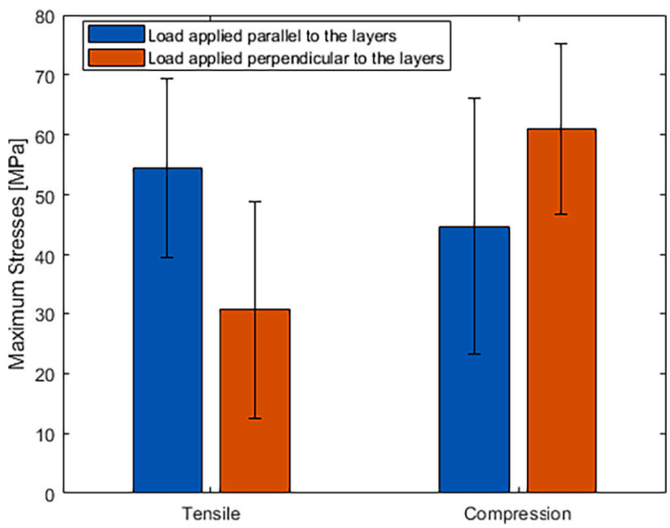

Fig. 1. Data acquisition (PLA material).

factors, but it can be said that it varies proportionally. For example, the authors have compared these directions for tensile [17–19] and compression [20–22] resistance. For the test, the authors printed samples from PLA material using Fused Deposition Modeling (FDM) technology, which as they mentioned, has a particularly big resulting anisotropy compared to the other technologies. The aggregated results in Fig. 1 show the differences between the directions, even though the results may differ significantly depending on the technological settings. Therefore, for optimizing the build orientation the emerged stress must meet these criteria.

To execute this kind of optimization regarding the compensation of layered structure, the first step is to assess the emerged force-flow in the functional engineering part. As Li et al. [23] concluded in their review paper, currently there is no existing de facto solution to visualize the force flow, but there are some guidelines, that can be used for the purpose. One of the most used methods is the Principal Stress Lines (PSL), which is a representation of the principal stress directions of any node inside the geometry. Based on the PSL, Kwok et al. [24] proposed a new algorithm that can be used for topology optimization, which results in a faster computation time, than some other solutions. Their fundamental approach is, that the material should be concentrated in the domain, where the PSL is the highest, and the unnecessary material can be removed from where the load-bearing is not justified. Therefore, the truss members of the optimized component ley along the PSLs as close as possible. Similarly, Sales et al. [25] in their research work used the PSL to adjust the printing parameters for better mechanical performance, via varying the infill structure and the extrusion width. However, as they also highlighted this concept needs further improvements, since they have only investigated the 2D shapes, thus the effect of layering was not considered. Tam and Mueller [26] developed a multi-axis 3D printer to produce the emerged geometry that has been optimized based on the PSL. By exploiting the movement of the robotic arm the struts of the parts can be deposited in three dimensions, therefore the adverse effect of anisotropy has been eliminated.

In this paper, an algorithm has been created that can determine the optimal printing orientation for better mechanical resistance in 3D.

2. Methods

2.1. Classification of the stress directions

As was mentioned in the Introduction chapter, several research works focused on obtaining the anisotropic behavior of the AM parts, based on mechanical measurements. In this paper, the proposed algorithm aims to find the best printing orientation that best resists the tensile loads. Therefore, as a first step, the relevant measurement data about the tensile test results were collected to test the procedure. The results of three independent research works have been used [17–22], each of them obtained the anisotropic behavior of the samples printed from PLA raw material utilizing the FDM technique.

Summarizing the results, it can be stated, that the part with an applied tension load that parallels the layers, or compressed perpendicular to the layers has higher resistance than those with the same loads in the opposite direction. Fig. 2. concludes the fundamental concept.

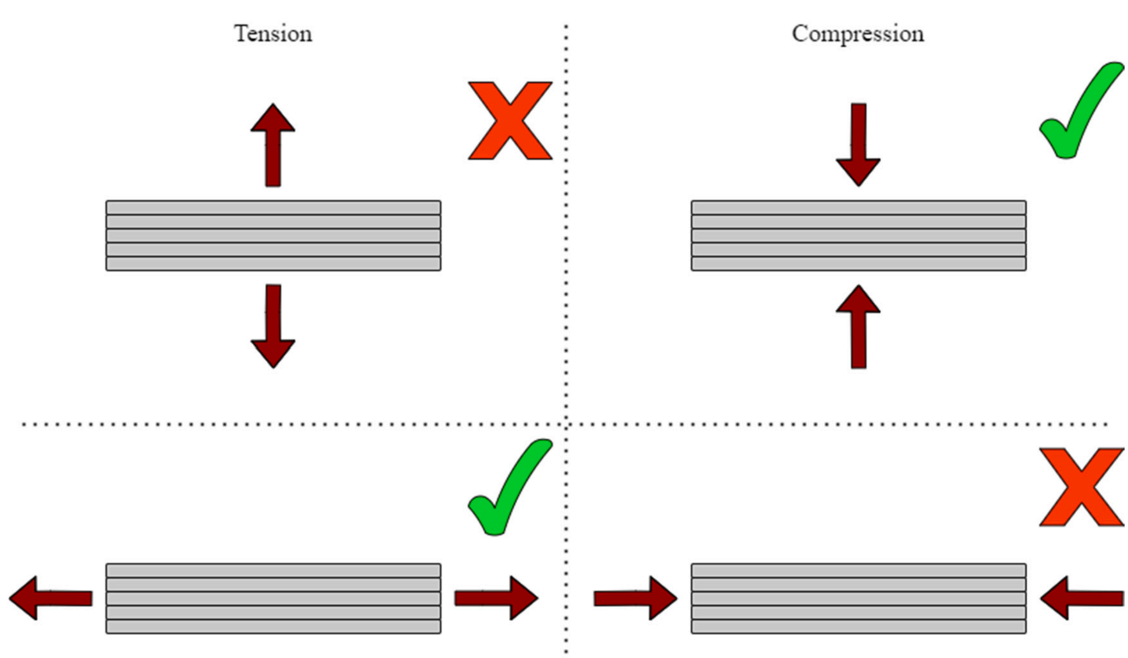

Fig. 2. Representation of different load cases.

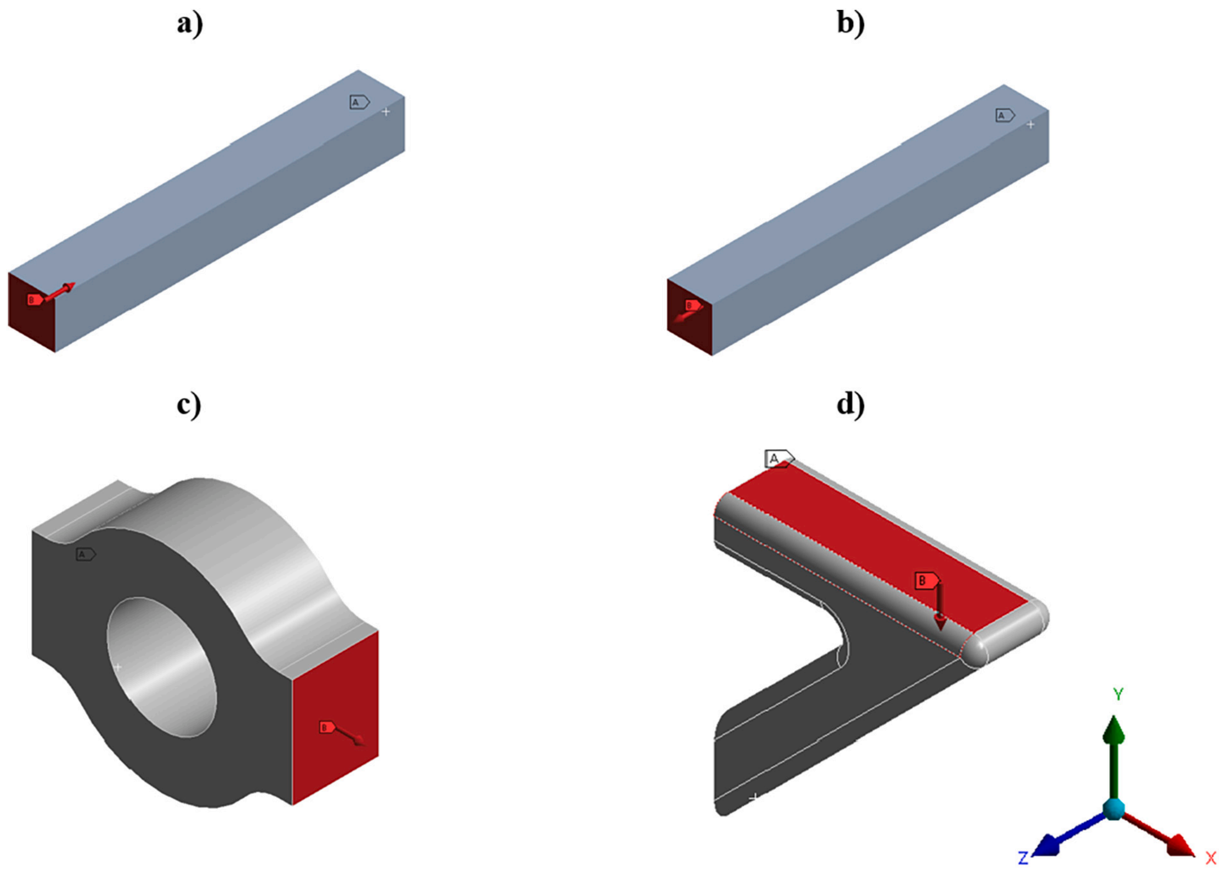

Fig. 3. Investigated geometries and simulation setup **a)** beam with compression load, **b)** beam with tensile load, **c)** Hinge, and **d)** Bracket.

2.2. FEA simulation

To define the Principal Stress (PS) directions and magnitudes inside the parts Ansys 2021 R2 Finite Element Analysis software was used. The selected material model was a homogeneous, isotropic, linear, elastic PLA (modulus of elasticity 2.1 GPa, Poisson ratio 0.3) since the purpose of the proposed algorithm was to provide a solution for a variety of AM technologies and raw materials, and the actual magnitude of the emerged stresses is less important than the ratio between the worst and optimal solutions. The anisotropy is the result of the process, not the property of the raw material. Thus, the assessment of the stress field can be performed on an isotropic material. As a result of the simulation, the Principal Stresses for each node that builds up the mathematical model have been evaluated. The Principal Stresses is the solution for the eigenvalue problem, where the coordinate system is rotated in a way, that the shear stresses are fallen out from the stress tensor matrix (Eq. (1)).

$$\begin{bmatrix} \sigma_{xx} & \sigma_{xy} & \sigma_{xz} \\ \sigma_{yx} & \sigma_{yy} & \sigma_{yz} \\ \sigma_{zx} & \sigma_{zy} & \sigma_{zz} \end{bmatrix} \begin{bmatrix} X_1 \\ X_2 \\ X_3 \end{bmatrix} = \lambda \begin{bmatrix} X_1 \\ X_2 \\ X_3 \end{bmatrix} \tag{1}$$

Four different geometries were investigated in this study. The first and second ones are simple prismatic beams, with compression and tensile loads. On one of their faces, a Fix Support and a Force on the opposite face have been applied. The magnitude of this force was 1 kN in the Z direction for the beam with tensile stresses, and −1 kN in the Z direction for the beam with compression stresses. The third is a simplified hinge component, with a cylindrical hole in the middle. For this geometry, a Fix Support on the left side, and a surface Force on the right side were applied. The direction of the force was defined by its components: 5 kN in the X direction and 0 N in the Y and Z direction, creating tension within the component. The fourth one is an angle bracket. The primitive of this shape is frequently used for testing the generative design techniques and comparing the different resulting organic shapes. Similarly, a Fix Support was applied on one of its sides, and an applied Force on the top surface. The components of this force were −5 kN in the Y direction, and 0 N in the other two directions. The geometry of the investigated parts and boundary conditions for the FEA simulations are presented in Fig. 3.

The results of the simulations have been exported in a CSV file format and for further investigations, MATLAB R2019b software has been used. The necessary input variables for the investigation were the Principal Stress magnitude for the three orthogonal axes and the corresponding Euler rotation angles, which define the direction of each of the Principal Stresses. Euler angles assign the orientation of maximum, middle, and minimum principal stresses to the global coordinate system, X-Y-Z correspondingly.

2.3. Euler rotation

In this study, the well-known and proven Euler transformation was used. The orientation of any rotated rigid body can be described as the initial fixed Descartes coordinate system. The process consists of three consecutive elementary rotations according to the Proper Euler angles (z-x-z, x-y-x, y-z-y, z-y-z, x-z-x, y-x-y) or the Tait-Bryan angles (x-y-z, y-z-x, z-x-y, x-z-y, z-y-x, y-x-z). In this paper, the x-y-z order has been used, since MATLAB has a built-in function for performing this kind of rotation.

2.4. Proposed algorithm

After importing the FEA simulation results, the first step is to perform the Euler rotation of the unit vector matrices (three orthogonal vectors) representing the orientation of the Principal Stress directions for each

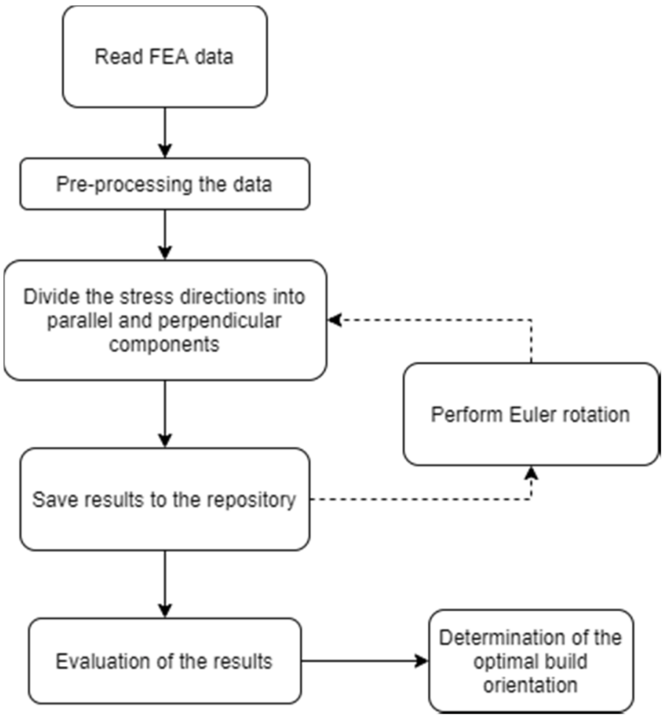

Fig. 4. Proposed algorithm.

node. As the result of the numerical simulation, Ansys and every FEA software define the tensile stress as a positive value and the compression stress is represented as a negative value for each node inside the body. Here, the anisotropic behavior of the part can be defined for the algorithm. As is discussed in detail in the Introduction, the parts resist fewer tension loads applied perpendicular to the build tray, but the compression loads can apply in this direction, since, the effect of layers is minimal. Here, purely the material bears the loads, and the adhesion/cohesion boundary is insignificant. The proposed algorithm is according to Fig. 4.

The calculations regarding the maximum compression and tensile stresses for the parallel and perpendicular directions are presented in the evaluation section below.

2.5. Evaluation method

Compliance with the pre-defined conditions must be evaluated. To find the most suitable orientation, the algorithm checks many possible options. For that, the rotation of the part according to the Euler angles was executed in the range of 0–180 degrees, with a 10-degree resolution for each axes (X, Y, and Z correspondingly). Therefore, overall 6859 cases were investigated. In each rotated position the direction and the magnitude of each Principal Stress must be linked together. For the evaluation, the absolute value of the angles between the Principal Stress directions and the build tray must be assessed (Fig. 5.a). Here, the plane that fits on the x-y axes of the global coordinate system represents the build tray. Secondly, by knowing these angles (between the build tray and the Principal Stress direction vectors) the components of the vectors can be determined. As with the orientation optimization, it is important to determine the projections of the vectors perpendicular to and parallel to the printer tray (Fig. 5.b). By the PS method, three orthogonal stress components are defined at each node, thus the calculated projections must be summarized at each node. The tensile stresses are represented with positive, and the compression stresses with a negative value. Combining the individual vectors, more precisely their projections, the characteristic load of interest for the study for each node can be obtained.

The Eqs. (2) and (3) summarize how the algorithm takes into account the two main objectives.

$$f_1 = -\frac{1}{n}\sum_{i=1}^{n}(Tension_{x,i}) \quad (2)$$

$$f_2 = \frac{1}{n}\sum_{i=1}^{n}(Compression_{z,i}) \quad (3)$$

Where, f_1 is the number of tension stresses parallel to the layers, f_2 is the amount of compression stresses perpendicular to the layers, and n is the number of nodes inside the investigated domain. For the study, only the average of the X-direction projections of the tensile stresses ($Tension_x$) at each node is relevant, and similarly, only the Z-direction projections of the compression stresses ($Compression_z$) have to be assessed. The basic assumption is that if a particular stress component given in one direction is maximal, it means that the other component of the same stress is minimal and vice versa. The (−1) multiplier is needed to reconcile the two functions later to implement the multi-objective optimization.

The optimal printing orientation is maintained when the lowest possible tension is applied perpendicular to the printing plane and the compression load parallel to the layers is minimal. As well as the compression perpendicular and tension parallel does not exceed the bulk and yield strength of the material. After the definition of the load characteristics, the algorithm must find the orientation, where the value of the average compression stresses along the print direction (f_2) is

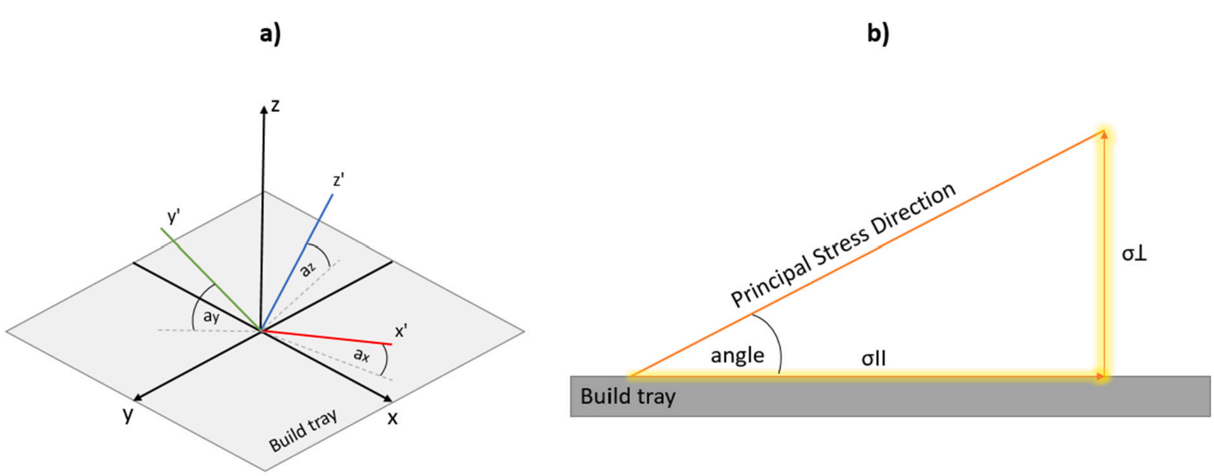

Fig. 5. a) Angles between the Principal Stresses and the build tray, and **b)** components of the Principal Stresses.

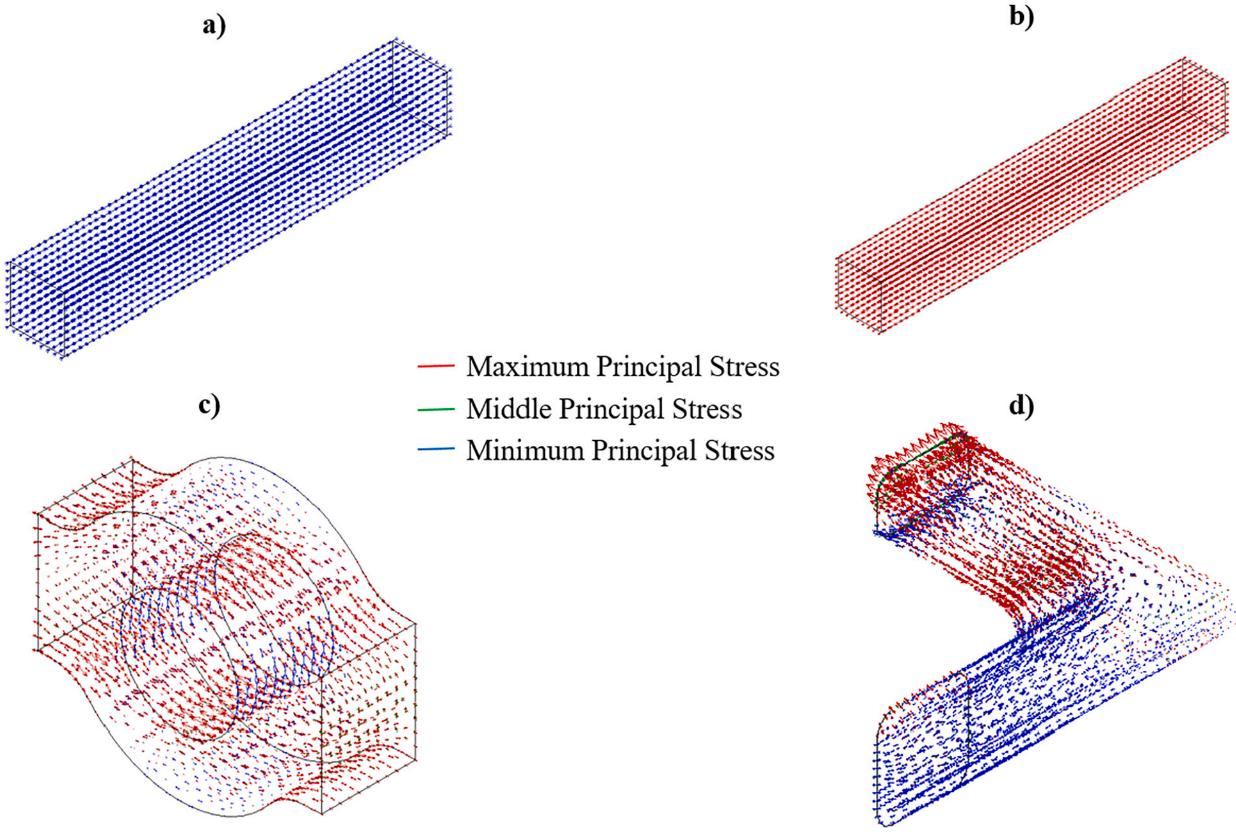

Fig. 6. Emerged Principal Stress lines inside **a)** beam with compression load, **b)** beam with tensile load, **c)** Hinge, and **d)** Bracket.

minimal and the average value of the maximal tension stresses along the build tray's plane (parallel with the layers) are maximal, which in this case means also minimal due to the negative multiplier (f_1). Due to the adverse effects shown above, it is primarily important to avoid applying tension load perpendicular to the layers. It can either be an acceptably low emerged tension stress or (negative) compression. For the algorithm to determine the best case among the combinations and to initialize the multi-objective optimizations, firstly the "*No Preference Method*" relation (4) can be used:

$$\begin{aligned} &Minimize: && \left\| f(\vec{x}) - z^{ideal} \right\| \\ &\text{subject to}: && \vec{x} \in S \end{aligned} \tag{4}$$

where $\vec{x}$ are all the elements inside of an S feasible region, and z^{ideal} is the theoretical value, which suits the conditions the best, but unattainable. Since z^{ideal} is not a feasible solution, the algorithm should aim to find the print orientation which is closest to this point.

Assume that one has sufficient information and experience to determine the preferences. Then, from the objectives, it is possible to determine, based on proportionality, which one is more relevant and which one is less. Thus the No Preference method can be replaced by a Priori Weighting method. The generalized relation is (5), where w_i is the weighting factor for the objectives.

$$\begin{aligned} &Minimize: && \sum_{i=1}^{k} w_i f_i(\vec{x}) \\ &\text{subject to}: && x \in S \\ &\text{where}: && w_i \geq 0 \text{ for all } i = 1, \ldots, k \text{ and} \\ & && \sum_{i=1}^{k} w_i = 1 \end{aligned} \tag{5}$$

3. Results and discussion

As a result of the numerical simulations, all of the Principal Stress directions have been determined for each node. For representation purposes, the program highlights the Maximum principal stress with red arrows, the minimal principal stress with blue arrows, and the middle principal stresses with green arrows (Fig. 6.). It can be seen that for the two beams only compression or tension stresses have been formed, respectively to the direction of the applied force.

The initial orientation is theoretically the best for the beam with compression load geometry, since it can be read from the figures that all of the compression PS lines are parallel with the Z (print) direction. Therefore, it is expected that the algorithm will find this as optimum. However, the initial orientation of the beam with tensile load is the worst, therefore the algorithm must rotate it 90 degrees around at least one axes, to make it lay down on the build tray. In this case, the load direction turns parallel to the layers, which means that the part becomes more loadable.

For the Hinge geometry, the force flow represented by the Principal Stresses is also rather simple, the best printing orientation, or the orientation close to the optimum could be determined easily without the algorithm. However, the bracket geometry has both significant tensile and compression stresses, and the emerged force flow is rather complex. Therefore, the assessment of the adverse effect and the most appropriate print orientation is more challenging. In this case, the load direction.

Confrontational plots can be seen in Figs. 7–10 related to the results. The computational time for each tested geometry was under 15 min. However, this time is highly affected by the angle resolution. Table 1. contains the computational time of the tested geometries with different angle resolutions.

On the Figures below the points represent the possible variations in the search space. As per the multiple objective optimization requirements, the Pareto optimal set has been found, since the set of

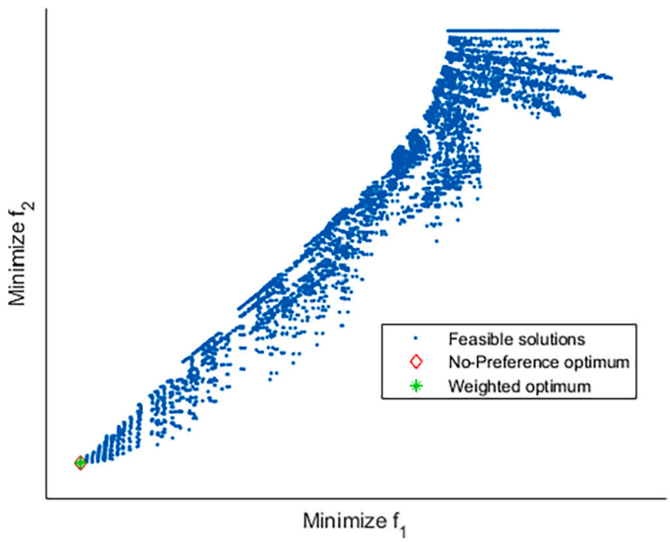

Fig. 7. Results for beam with compression loads.

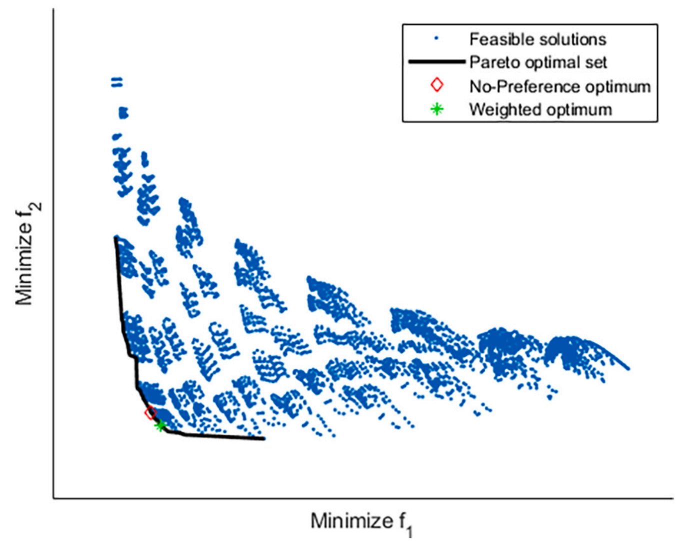

Fig. 9. Results for hinge.

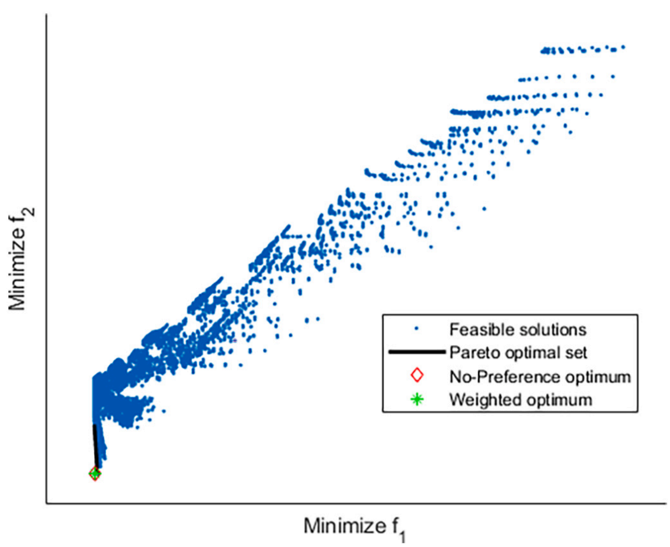

Fig. 8. Results for beam with tensile load.

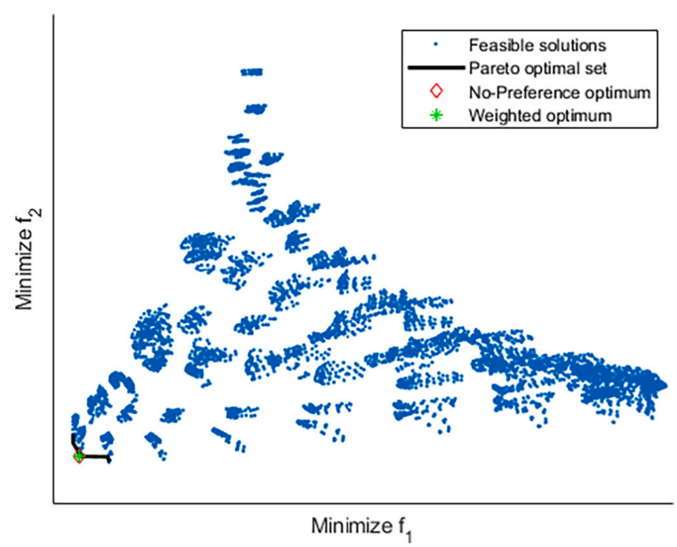

Fig. 10. Results for bracket.

feasible solutions dominates over the others. It can be stated, that for all shapes a set of possible orientations are dominant over the others, thus the selection among them can be performed. Based on the optimization objective, the resulting stress values for the best orientations should be located around the lower-left corner. In all cases, it must be borne in mind that the stress generated never exceeds the maximum permissible limit value. Therefore, if a load pushes the limit of component tolerances, the extremums of the Pareto optimal may no longer meet the requirements.

Based on the numerical result each solution vector of the Pareto front meets the boundary condition, e.g. none of the adverse stresses are exceeding the limits. Therefore, the selection can be made by the decision-maker. At first, it is assumed, that the decision-maker does not have any prior information about the goal objective. Therefore, the solution, which best fulfills the requirements is selected by using the No Preference Method to select the best orientation from the Pareto optimal set. The introduced relation (4) can be extended and solved as follows Eq. (6):

Table 1
Computational time of the tested cases.

		Computational time (*sec*)			
		Beam with compression	Beam with tension	Hinge	Bracket
Angle resolution (deg)	10	731.14	736.8	494.62	891.43
	30	36.56	36.84	24.73	44.58
	45	11.84	11.51	8.34	14.37
	60	6.11	5.97	4.14	7.47
	90	2.83	2.83	2.02	2.98

$$Minimize: \quad \sum_{i=1}^{k}\left(f_i(\vec{x}) - z^{ideal}\right)^p\Bigg)^{\frac{1}{p}} \quad \text{subject to:} \quad \vec{x} \in S \tag{6}$$

The location of z^{ideal} has been defined by the lowest feasible adverse stresses for all geometries. The value for p is selected in most cases as $p =$ 1, 2, or ∞. Since the dominant objective vectors may form a non-convex problem the value 2 has been selected, as it serves the requirements the

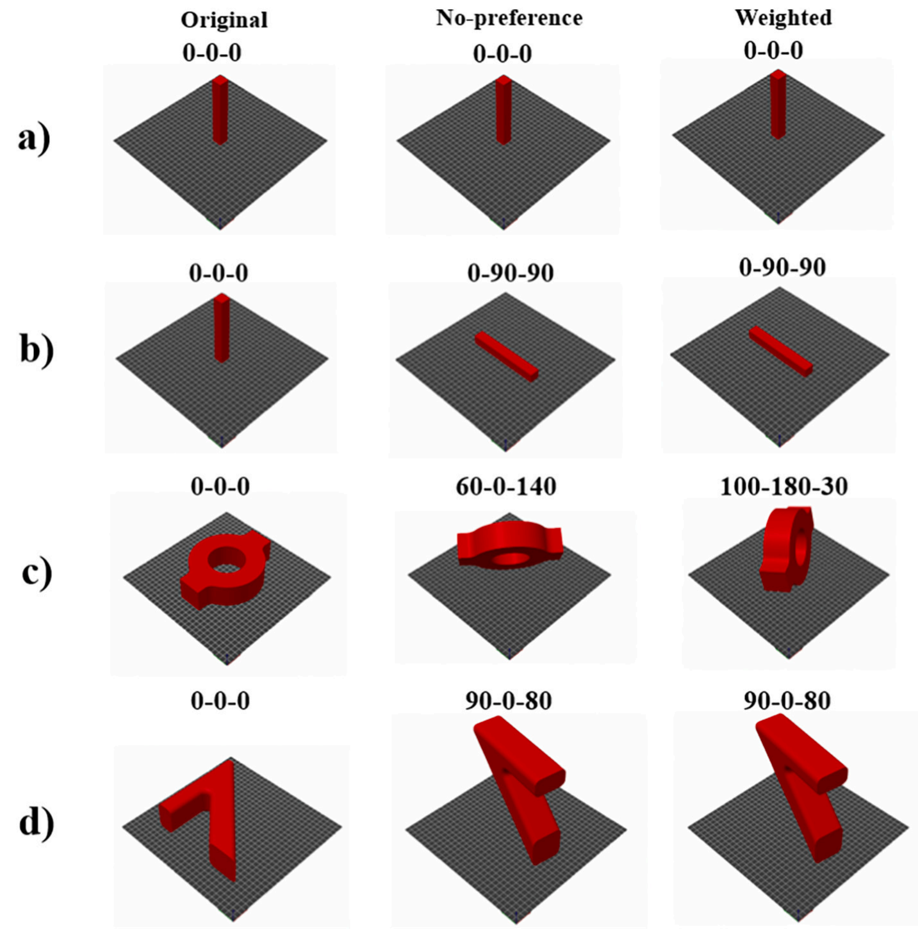

Fig. 11. Representation of the rotated orientations **a)** beam with compression load, **b)** beam with tensile load, **c)** hinge, and **d)** bracket.

best.

According to the second optimization method, by assuming some inequality between the objectives the weighting method was used. Since in this particular optimization problem, there are only two objectives to aggregate, the relation for weighted optimum (5) can be simplified to Eq. (7).

$$\begin{aligned} Minimize: \quad & z^* = (1-w)f_1(\vec{x}) + wf_2(\vec{x}) \\ \text{where}: \quad & 0 \le w \le 1 \end{aligned} \tag{7}$$

In this Eq. (7), f_1 refers to the first objective, that the inverse value of the tensile stresses parallel to the layers must be minimized and f_2 is that the compression stresses perpendicular to the layers must be minimized. For the second objective, remember that the compression stresses are represented as negative numbers, thus the most minimal value means the maximum emerged compression stress in that direction. To select the value for w, the collected reference data has been used for FDM technology. From their combined results it can be determined, that the comprehensive ratio of the loads in different directions is 1.83 for tensile and 1.33 is for compression. It means that the part created by this technology is more sensitive to the tensile stress direction than the compression's direction. Quantifying this sensitivity, w was chosen to be 0.58 to proportionally express the more dominant role of f_1 in the optimization.

On the plots of the results of the two beam geometries, it can be seen that depending on the applied force direction the tension or the compression stresses are negligible. Because of this, the two objective optimizations could be reduced to one objective for both cases, and the optimum is the orientation where significant stress (tension or compression) is the largest in absolute terms. This is most pronounced at the beam with a compression load, as there is a privileged direction that perfectly satisfies both aspects so this orientation always dominates over the others.

On the plots of the Hinge and Bracket shapes, it can be seen that the result points are locally condensed in some places. This can be explained by the fact that in a given resolution but all orientations have been examined, whereas the results of certain orientations do not differ significantly from the point of view of the study, they can be considered equivalent results. The reason why these obtained points do not overlap can be explained by the fact that the result of the simulation may be slightly different on both sides of a symmetric piece due to the inaccuracy of the mesh and slight rounding errors in the calculation.

Since the Hinge's load condition was rather simple, mainly tension stresses have occurred, but due to the hole in the middle, some remarkable compression has emerged. A few clusters can be seen in Fig. 7. since due to the semi-symmetric geometry and simple load case, some positions are equivalent. The most favourable orientation based on the No Preference Method and according to the Euler transformation is 60–0-140, compared to the original state (0-0-0), X-Y-Z respectively. The best rotation based on the weighted sum method is the same 100-180-30.

The results of the bracket geometry also show the island-like point concentration, which is the result of the same effect. Due to the more complex emerged stress states the part has less symmetry plane, therefore, the distribution in the objective space is more scattered. It can be said, that there are printing orientations that cause significantly worse mechanical resistance of the part than some others. The best orientation for both according to the No Preference Method and the Weighted Sum Method is with the Euler angles 90-0-80. As the weighting factor used is

Table 2
Numerical results of the favourable stress components.

	Original		No-preference		Weighted	
	σ_{II} (tens.)[MPa]	$\sigma_{\perp}$ (comp.)[MPa]	σ_{II} (tens.)[MPa]	$\sigma_{\perp}$ (comp.)[MPa]	σ_{II} (tens.)[MPa]	$\sigma_{\perp}$ (comp.)[MPa]
Beam with compression load	~0	−12.29	~0	−12.29	~0	−12.29
Beam with tensile load	~0	~0	12.29	~0	12.29	~0
Hinge	8.01	−0.433	7.98	−1.89	7.71	−2.55
Bracket	2.88	−0.461	3.33	−3.61	3.33	−3.61

Table 3
Numerical results of the adverse stress components.

	Original		No-preference		Weighted	
	$\sigma_{\perp}$ (tens.)[MPa]	σ_{II} (comp.)[MPa]	$\sigma_{\perp}$ (tens.)[MPa]	σ_{II} (comp.)[MPa]	$\sigma_{\perp}$ (tens.)[MPa]	σ_{II} (comp.)[MPa]
Beam with compression load	~0	~0	~0	~0	~0	~0
Beam with tensile load	12.29	~0	~0	~0	~0	~0
Hinge	0.92	−2.59	1.16	−1.83	2.37	−0.65
Bracket	1.71	−3.63	0.33	−0.58	0.33	−0.58

not particularly significant, this orientation fits both methods. In Fig. 11 the representation of the original and the rotated positions can be seen.

It can be seen that for all geometry some other similar orientations can all be suitable, but due to the inaccuracy of the simulation results, the algorithm will always find a position that is minimally but dominant compared to the others. For example, in the case of the Bracket, the algorithm found the optimal position, but by rotating it around the printing direction (z-axis) a similarly favourable orientation can be found. The quantified results for the orientations obtained in the favourable and adverse directions are given in the Table 2 and Table 3. Here the favourable stress components correspond to the load cases marked with a green tick in Fig. 2, and the adverse stress components are according to the load cases marked with red X.

Since the optimization objectives were to maximize the favourable stresses, consequently this means that the adverse stresses will be minimalized, as they are perpendicular to the investigated objectives. As can be seen from the results of the two beams, only one of the objectives was significant and at the optimal orientation. These have the largest possible numerical values (in absolute terms) for the optimal position, and for the adverse components, the values are minimal. For the hinge geometry, the original orientation would be the best for the tension stress objective, but with the rotation along the longitudinal axis, the secondary objective was improved, while the first objective was just barely degraded. At the bracket, both objectives were improved with the appropriate orientation.

4. Conclusion

As several previous research have presented, additively manufactured components have significant anisotropy. The mechanical performance of the parts can significantly be improved by choosing the right printing orientation, as this minimizes the detrimental effect of layering. In this paper an algorithm has been developed, which aims to find a build orientation, where the adverse load cases are reduced, therefore the expected load resistance can be increased. Based on results, that can be associated with the anisotropy of orthogonal main directions, the optimization relation can be determined. The necessary steps of the algorithm are the following:

1. Perform a numerical simulation to get the Principal Stress vectors inside the part under a specific load case.
2. Breaking down the obtained result directions into components to obtain the favourable and adverse degree of tension or compression for each node examined.
3. By rotating according to the Euler angles, check the stress magnitudes according to the point above at each position.
4. From the obtained results a set of possible best orientations can be determined.

Of the four geometries examined, the optimal orientation of the two beams can be easy without calculation, therefore, it proves the reliability of the algorithm. However, in the case of the other two complex shapes, without calculation there is no close estimation, so the usefulness of the presented method is proved. In future work, the proposed algorithm must be extended with a feature recognition function, as with the Principal Stress approach, only the emerged tension and compression at the concentrated points of the optimization domain was investigated. However, for highly complex shapes with interrupted surfaces, the shear stresses cannot be neglected.

Declaration of competing interest

The authors declare that they have no known competing financial interests or personal relationships that could have appeared to influence the work reported in this paper.

Acknowledgement

Application Domain Specific Highly Reliable IT Solutions” project has been implemented with the support provided from the National Research, Development and Innovation Fund of Hungary, financed under the Thematic Excellence Programme TKP2020-NKA-06 (National Challenges Subprogramme) funding scheme.

References

[1] Jiang J. A novel fabrication strategy for additive manufacturing processes. J. Clean. Prod. 2020;272:122916. https://doi.org/10.1016/j.jclepro.2020.122916.
[2] Jiang J, Ma Y. Path planning strategies to optimize accuracy, quality, build time and material use in additive manufacturing: a review. Micromachines. 2020;11. https://doi.org/10.3390/MI11070633.
[3] Wi K, Suresh V, Wang K, Li B, Qin H. Quantifying quality of 3D printed clay objects using a 3D structured light scanning system. Addit. Manuf. 2020;32:100987. https://doi.org/10.1016/j.addma.2019.100987.
[4] Dine A, Vosniakos GC. On the development of a robot-operated 3D-printer. Procedia Manuf. 2018. https://doi.org/10.1016/j.promfg.2018.10.004.
[5] Mishra V, Ayas C, Langelaar M, Van Keulen F. Simultaneous topology and deposition direction optimization for wire and arc additive manufacturing. Manuf. Lett. 2021. https://doi.org/10.1016/j.mfglet.2021.05.011.
[6] J.S. Shim, J. Kim, H. Jeong, J. Choi, Printing accuracy , mechanical properties , surface characteristics , and microbial adhesion of 3D-printed resins with various printing orientations, J. Prosthet. Dent. (n.d.) 1–8. doi:10.1016/j. prosdent.2019.05.034.

[7] Pandey PM, Thrimurthulu K, Reddy NV. Optimal part deposition orientation in FDM by using a multicriteria genetic algorithm. Int. J. Prod. Res. 2004;42: 4069–89. https://doi.org/10.1080/00207540410001708470.
[8] Cheng W, Fuh JYH, Nee AYC, Wong YS, Loh HT, Miyazawa T. Multi-objective optimization of part-building orientation in stereolithography. Repid Prototyp. J. 1995;1:12–23.
[9] Lockett H, Ding J, Williams S, Martina F, Lockett H. Design for Wire + arc additive manufacture : design rules and build orientation selection. J. Eng. Des. 2017;4828. https://doi.org/10.1080/09544828.2017.1365826.
[10] Leutenecker-Twelsiek B, Klahn C, Meboldt M. Considering part orientation in Design for Additive Manufacturing. Procedia CIRP. 2016;50:408–13. https://doi.org/10.1016/j.procir.2016.05.016.
[11] Hong C, Nguyen P, Choi Y. Concurrent density distribution and build orientation optimization of additively manufactured functionally graded lattice structures. Comput. Des. 2020;127:102884. https://doi.org/10.1016/j.cad.2020.102884.
[12] Barbero EJ. Finite element analysis of composite materials using ansys, 2nd editio. CRC Press 2013. https://doi.org/10.1201/b16295.
[13] Skrzypek JJ, Ganczarski AW. Mechanics of anisotropic materials. Springer; 2015.
[14] Ma G, Li Z, Wang L, Wang F, Sanjayan J. Mechanical anisotropy of aligned fiber reinforced composite for extrusion-based 3D printing. Construct. Build.Mater. 2019;202:770–83. https://doi.org/10.1016/j.conbuildmat.2019.01.008.
[15] Torrado AR, Shemelya CM, English JD, Lin Y, Wicker RB, Roberson DA. Characterizing the effect of additives to ABS on the mechanical property anisotropy of specimens fabricated by material extrusion 3D printing. Addit Manuf 2015;6: 16–29. https://doi.org/10.1016/j.addma.2015.02.001.
[16] Ren Y, Tariq H, Liu H, Zhao L, Cui X, Shen Y. Study of microstructural and mechanical anisotropy of 7075 Al deposits fabricated by cold spray additive manufacturing. Mater. Des. 2021;212:110271. https://doi.org/10.1016/j.matdes.2021.110271.
[17] Hanon M, Dobos J, Zsidai L. The influence of 3D printing process parameters on the mechanical performance of PLA polymer and its correlation with hardness. Procedia Manuf. 2021;54:244–9. https://doi.org/10.1016/j.promfg.2021.07.038.
[18] Yao T, Deng Z, Zhang K, Li S. A method to predict the ultimate tensile strength of 3D printing polylactic acid (PLA) materials with di ff erent printing orientations. Compos. Part B 2019;163:393–402. https://doi.org/10.1016/j.compositesb.2019.01.025.
[19] Wang Y, Li S, Yu Y, Xin Y, Zhang X, Zhang Q, Wang S. Lattice structure design optimization coupling anisotropy and constraints of additive manufacturing. Mater. Des. 2020;196:109089. https://doi.org/10.1016/j.matdes.2020.109089.
[20] Gradinaru S, Tabaras D, Gheorghe D, Zamfir R, Vasilescu M, Grigorescu G, Cristescu I. Analysis of the anisotropy for 3D printed PLA parts usable in medicine, UPB sci. Bull. Ser. B Chem. Mater. Sci. 2019;81.
[21] Manufactured A, Fused U, Modelling D, Baker AM, Mccoy J. Measurement and Modelling of Thermal and Mechanical Anisotropy of Parts Measurement and Modelling of Thermal and Mechanical Anisotropy of Parts Additively Manufactured Using Fused Deposition Modelling (FDM). 2017. https://doi.org/10.12783/shm2017/13917.
[22] Perkowski C. Tensile-compressive asymmetry and anisotropy of fused deposition modeling PLA under monotonic conditions. University of Central Florida; 2019.
[23] Li S, Xin Y, Yu Y, Wang Y. Design for additive manufacturing from a force-flow perspective. Mater. Des. 2021;204:109664. https://doi.org/10.1016/j.matdes.2021.109664.
[24] Kwok TH, Li Y, Chen Y. A structural topology design method based on principal stress line. CAD Comput. Aided Des. 2016;80:19–31. https://doi.org/10.1016/j.cad.2016.07.005.
[25] Sales E, Kwok T, Chen Y. Function-aware slicing using principal stress line for toolpath planning in additive manufacturing. J. Manuf. Process. 2021;64:1420–33. https://doi.org/10.1016/j.jmapro.2021.02.050.
[26] Tam KM, Mueller CT. Additive manufacturing along principal stress lines, 3D print. Addit. Manuf. 2017;4. https://doi.org/10.1089/3dp.2017.0001.

Nomenclature

$\sigma_{xx}; \sigma_{yy}; \sigma_{zz}; \sigma_{xy}; \sigma_{xz}; \sigma_{yx}; \sigma_{yz}; \sigma_{zx}; \sigma_{zy}$: Elements of stress tensor matrix
λ: Eigenvalue
$X_1; X_2; X_3$: Elements of Eigenvector
$a_x; a_y; a_z$: Angles between the build tray and the principal stress vectors
f_1: First objective; amount of tension stresses parallel to the layers
f_2: Second objective; amount of compression stresses perpendicular to the layers
n: Number of investigated nodes
$Tension_x$: X-direction projections of the tensile stresses
$Compression_z$: Z-direction projections of the compression stresses
z^{ideal}: Theoretically best orientation
S: Feasible region
w: Weighting factor
σ_{II}: Stress parallel to the build tray
$\sigma_{\perp}$: Stress perpendicular to the build tray